

Reaction of niobium and tantalum neutral clusters with low pressure, unsaturated hydrocarbons in a pickup cell: From dehydrogenation to Met-Car formation

S.-G. He and Y. Xie, F. Dong and E. R. Bernstein

Citation: *The Journal of Chemical Physics* **125**, 164306 (2006); doi: 10.1063/1.2360278

View online: <http://dx.doi.org/10.1063/1.2360278>

View Table of Contents: <http://aip.scitation.org/toc/jcp/125/16>

Published by the *American Institute of Physics*

COMPLETELY

REDESIGNED!



**PHYSICS
TODAY**

Physics Today Buyer's Guide
Search with a purpose.

Reaction of niobium and tantalum neutral clusters with low pressure, unsaturated hydrocarbons in a pickup cell: From dehydrogenation to Met-Car formation

S.-G. He and Y. Xie

*Department of Chemistry, Colorado State University, Fort Collins, Colorado 80523-1872*F. Dong and E. R. Bernstein^{a)}*Department of Chemistry, Colorado State University, Fort Collins, Colorado 80523-1872 and NSF ERC for Extreme Ultraviolet Science and Technology, Colorado State University, Fort Collins, Colorado 80523-1872*

(Received 31 July 2006; accepted 12 September 2006; published online 24 October 2006)

Neutral niobium and tantalum clusters (Nb_n and Ta_n) are generated by laser ablation and supersonic expansion into a vacuum and are reacted in a pickup cell with various low pressure (~ 1 mTorr) unsaturated hydrocarbons (acetylene, ethylene, propylene, 1-butene, 1,3-butadiene, benzene, and toluene) under nearly single collision conditions. The bare metal clusters and their reaction products are ionized by a 193 nm laser and detected by a time of flight mass spectrometer. Partially and fully dehydrogenated products are observed for small ($n \leq m$) and large ($n \geq m$) neutral metal clusters, respectively, with m ranging from 2 to 5 depending on the particular hydrocarbon. In addition to primary, single collision products, sequential addition products that are usually fully dehydrogenated are also observed. With toluene used as the reactant gas, carbon loss products are observed, among which Nb_8C_{12} and Ta_8C_{12} are particularly abundant, indicating that the Met-Car molecule M_8C_{12} can be formed from the neutral metal cluster upon two collisions with toluene molecules. The dehydrogenation results for low pressure reactions are compared with those available from previous studies employing flow tube (high pressure) reactors. Low pressure and high pressure cluster ion reactions are also compared with the present neutral metal cluster reactions. Reactions of unsaturated hydrocarbons and metal surfaces are discussed in terms of the present neutral cluster results. © 2006 American Institute of Physics. [DOI: 10.1063/1.2360278]

I. INTRODUCTION

Reactivity of both neutral and charged nanometer sized transition metal clusters has been extensively studied^{1,2} since the pioneering work of Smalley and co-workers.^{3–5} Charged clusters are in principle readily controlled and manipulated with electric and magnetic fields, and can be studied under mass selective conditions. In contrast, neutral clusters are difficult to control and usually must be ionized for detection.

Two approaches have been taken to the study of neutral cluster reactivity. In the first approach,⁴ clusters formed in a narrow channel expand into a directly coupled fast flow (flow tube) reactor, in which metal clusters (M_m) undergo many collisions with both reactant(s) (A , etc.) and bath (e.g., He) gas. After the reaction, the gases with ~ 1 –50 Torr pressure have a secondary expansion into the vacuum system for product analysis. In this instance, the heat of formation of the $M_nA \rightarrow M_nA^*$ process can be quickly dissipated by collisions with the bath gas and M_nA^* can be cooled and stabilized. In the second approach,⁶ the cluster reacts, after expansion into a vacuum system, with a low pressure (~ 1 mTorr) gas in a pickup cell under nearly single collision conditions. Scattering by gas molecules can destroy the molecular beam in this case and this approach is much less

employed than the first one. In the low pressure cell experiment, however, one can observe molecular decay products of M_nA^* ($M_nA^* \rightarrow B+C, B, C \neq A$) which may not be observable because of rapid cooling and stabilization of M_nA^* through collisions with the high pressure bath gas in the flow tube experiment. The sticking probability between neutral metal cluster and reactant gas molecule can also be evaluated for the pickup cell arrangement.⁷ Another advantage of the pickup cell arrangement is that an electric field can be applied to the cluster beam prior to its entrance into the reaction cell to deflect ions. This deflection is not easy to do in the high pressure flow tube system because the reactor is directly coupled to the cluster source, and as a result ionic clusters may contribute to the final neutral products.⁸

In the present study, a pickup cell is employed to study the reaction of neutral Nb_n and Ta_n clusters with unsaturated hydrocarbons. The reactions of neutral and charged Nb_n with various gases have been extensively studied due to niobium's single naturally abundant isotope and large specific reactivity.⁵ A brief review of the reactions of Nb_n with hydrocarbons is given below.

Reaction of benzene on neutral Nb_n was studied in a flow tube experiment by Pierre and El-Sayed^{9,10} and Zakin *et al.*¹¹ Products of the primary addition reaction, detected at very low ionization laser fluence ($\sim 50 \mu J/cm^2$), are $Nb_nC_6H_6$ (any n) and Nb_nC_6 ($n \geq 4$) with dehydrogenation

^{a)}Electronic mail: erb@lamar.colostate.edu

conversion probability (DCP) strongly dependent on n . Relatively low DCP is observed for $n=8$ and 10. Dehydrogenation was not observed for sequential addition reactions; in other words, $\text{Nb}_n\text{C}_{12}\text{H}_{12}$ and $\text{Nb}_n\text{C}_{12}\text{H}_6$, but not Nb_nC_{12} , are observed. Reaction of benzene with cationic Nb_n clusters¹² was also reported by Zakin *et al.* using a fast flow, high pressure reactor. The product distribution is similar to the one for the neutral Nb_n species, except that partial dehydrogenation is observed for $n \geq 3$ and a high DCP is observed for $n=4$. Pierre *et al.* also studied Nb_n reactivity toward several cyclic hydrocarbons;⁸ no product was observed with cyclohexane as a reactant but physisorbed and chemisorbed products are readily detected with unsaturated molecules (cyclohexene and 1,3-cyclohexadiene). Nb_n clusters have also been reacted with isobutane¹³ and ethylene¹⁴ in a fast flow reactor. Although products were observed in both experiments, the bare metal cluster depletion rate for ethylene is generally two orders of magnitude larger than the depletion rate for the saturated molecule, isobutane. In the reaction with ethylene, most of the primary and sequential addition products were only partially dehydrogenated. The depletion rate of Nb_8 and Nb_{10} with reactant ethylene was also small. A fast flow reactor was also employed to study the reaction of cationic Nb_n with saturated hydrocarbons n -butane and isobutane.¹⁵ Physisorbed and chemisorbed (partially dehydrogenated) products were observed for $n > 7$ and $n=1-7$, respectively.

The reactivity of cationic and anionic Nb_n has also been studied at low pressure in a Fourier transform ion cyclotron resonance (FT-ICR) spectrometer with various hydrocarbons.¹⁶⁻²¹ Products are observed with both saturated and unsaturated hydrocarbons, for small ($n \leq 7$) and all clusters, respectively. Reactions with C_2H_4 , C_6H_6 , and $\text{C}_6\text{H}_5\text{CH}_3$ are of particular interest for the present work and we will compare our results with a pickup cell for neutral Nb_n clusters with the FT-ICR results as is appropriate.

In contrast to the rather extensive investigation of niobium cluster chemistry for ions and neutrals, only a few studies of neutral tantalum clusters reacting with saturated hydrocarbons (ethane, propane, n -butane, isobutane, and neopentane) in a fast flow reactor (high pressure) are reported.^{22,23} The depletion rate of Ta_n clusters is found to be lower than the gas collision rate by two to three orders of magnitude, implying a weak reaction between Ta_n and saturated hydrocarbons.

In general, the dehydrogenation mechanism is particularly interesting in the above reactions at all pressures because a similar process is also found in catalytic reactions on metal surfaces.²⁴ Although the cluster system is suggested to be a good model for understanding surface catalytic behavior, the understanding of dehydrogenation of unsaturated hydrocarbons on small gas phase clusters is far from complete. Based on the high interaction energy (2–3 eV)²⁶ between charged metal atom/cluster and organic ligands (e.g., C_6H_6), a long lived collision complex formation and an effective temperature increase following intracluster vibrational energy redistribution of the interaction energy has been proposed by Bondybey and Beyer.²⁵ This mechanism was offered to explain their FT-ICR findings of dehydrogenation

products and is further supported by a ligand exchange experiment in which less dehydrogenation is usually observed if the cluster is solvated by inert gas atoms prior to reaction. The interaction energy between neutral clusters and unsaturated hydrocarbons is relatively small, ca. 0.5–1.5 eV based on surface and solid state measurements^{27,28} and calculations,²⁹ and as a result, the temperature increase for a neutral system is relatively small. This small cluster energy increase may not provide sufficient energy to overcome the barrier to dehydrogenation in a neutral cluster pickup experiment. Conditions (single collision) for a pickup cell and FT-ICR all are similar; moreover, a charged system may behave differently than a neutral one.

A comparison between the reaction results for neutral and ionic metal clusters (Nb_n) proves interesting in the fast flow experiments on Nb_n reactivity. With unsaturated hydrocarbons a few different dehydrogenation reaction mechanisms have been suggested. Pierre and El-Sayed⁹ proposed that size dependent dehydrogenation for $\text{Nb}_n/\text{C}_6\text{H}_6$ is driven thermodynamically with the number of NbC bonds maximized. Zakin *et al.*,¹¹ on the other hand, proposed that C–H bond breaking is an activated process with size selectivity arising from variations in the electronic and/or structural properties of the Nb_n clusters. The reaction of Nb_n with C_2H_4 has been suggested to be barrierless for both the association and dehydrogenation steps, and the extent of dehydrogenation is primarily determined by thermodynamic constraints.¹⁴ We reexamine these suggestions and ideas in the light of the new pickup cell reaction experiment reported below.

Transition metal containing carbide clusters ($M_n\text{C}_m$) are interesting species with potentially novel properties that could be used in practical applications, such as in semiconductors, and quantum and photovoltaic devices. These clusters are typically generated in a laser ablated metal plasma. Clusters with the $M_8\text{C}_{12}$ stoichiometry ($M=\text{Ti}, \text{Zr}, \text{V}, \text{Nb}$, etc.) (Met-Cars) are of particular interest.³⁰ Calculations for the structure of the Met-Cars generally confirm that the tetra-capped tetrahedron (T_d symmetry) is more stable than the pentagonal dodecahedron (T_h symmetry).³¹ Since we generate such species with benzene and toluene in a pickup system, we can ask if the $M_8\text{C}_{12}$ species generated in a plasma with CH_4 and the $M_8\text{C}_{12}$ species generated at much lower temperature in the pickup cell have the same structure. If both $M_8\text{C}_{12}$ species are in their lowest state and have the same structure, then reaction pathways found for the reactivity studies can provide useful information on the topologies of Met-Cars in general.

In this present work, reactions of neutral niobium and tantalum clusters with various unsaturated hydrocarbons in a low pressure pickup cell are explored and new product channels, not reported previously for flow tube, high pressure experiments, are observed. These results are compared with those from previous studies and reaction mechanisms for the generation of $M_n\text{C}_m\text{H}_x$ are discussed. When toluene is employed as a reactant gas for the M_n species, relatively intense hydrogen and carbon loss products $M_8\text{C}_{12}$ are observed. The reaction pathways suggested support at a T_d rather than a T_h topology for the $M_8\text{C}_{12}$ species, in agreement with theoretical predictions.

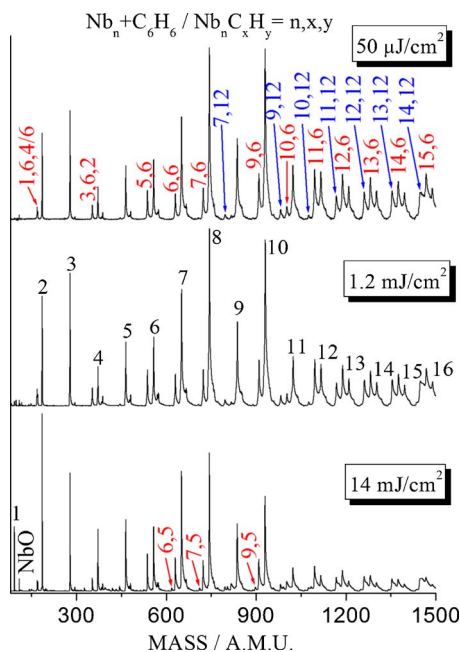


FIG. 1. Product distribution in the reaction of Nb_n with ~ 1 mTorr C_6H_6 in the pickup cell at three different 193 nm laser fluences. The weak shoulder on the high mass side of the main peaks is due to oxygen and carbon impurities. Similar impurity peaks are also present in all other spectra shown in this work.

II. EXPERIMENTAL PROCEDURES

The detailed instrumental apparatus employed in these studies has been discussed previously,³² and we will thus give only a brief outline of the experimental protocol. Nb_n/Ta_n clusters are generated by laser ablation [Nd^{3+} /yttrium aluminum garnet (YAG), 532 nm, 8–10 mJ/pulse, 5–8 ns duration] of Nb/Ta metal foil in the presence of high purity He (>99.995%) carrier gas. The clusters are formed in a 2 mm \times 33 mm cylindrical channel and expanded into a vacuum system with the carrier gas. The expansion generates a supersonic cluster beam. Ions in the cluster beam are deflected by applying a static electric field (200 V/cm, 2 cm long) downstream of the nozzle orifice. The neutral clusters in the beam pass through a 57 mm long pickup cell with a skimmer input (opening of 2 mm) and a plate hole (2 mm) exit. Reactant gas leaks into the pickup cell through a variable leak valve (Granville-Phillips). The cell gas pressure is measured by a precalibrated pressure transducer (MKS Baratron type 128). After collision and reaction in the gas cell, the cluster beam enters a time of flight ion source where a 193 nm laser beam (6–8 mm diameter, 10–15 ns duration) located 54 mm from the exit of the cell is used to ionize clusters and products. Ions are detected and signals are recorded as previously described³² by a time of flight mass spectrometer (TOFMS) with mass resolution of ± 1 amu at 500 amu.

III. RESULTS

Figure 1 presents the mass spectrum of niobium clusters Nb_n interacting with C_6H_6 in the pickup cell. The pressure of benzene in the cell is ca. 1 mTorr. The ionization laser wavelength is 193 nm. To investigate the laser fluence dependence

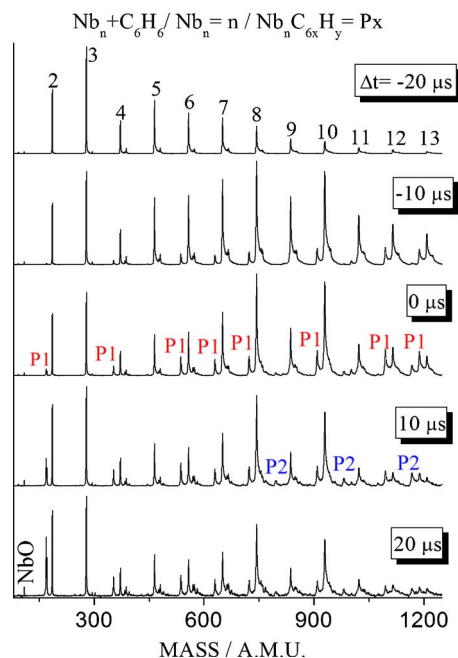


FIG. 2. Product distribution in the reaction of Nb_n with ~ 1 mTorr C_6H_6 in the pickup cell at five different relative delay times (Δt) for the ionization laser (193 nm, $190 \mu J/cm^2$) pulse with respect to the ablation laser pulse.

of the mass spectra for the system, the laser fluence is varied over the range of $< 50 \mu J/cm^2$ to $14 mJ/cm^2$. The figure shows that at less than ca. $1 mJ/cm^2$ the spectra are stable and not dependent on laser fluence. At high fluence, ca. $15 mJ/cm^2$, weak photochemical products (e.g., $Nb_n C_5$ from $Nb_n C_6$) are observed. The major products of this reaction in the pickup cell low pressure experiment are fully dehydrogenated ($Nb_n C_6$) species. This result is different from that in the high pressure flow tube reactor for which the nondehydrogenated products ($Nb_n C_6 H_6$) usually have comparable intensities to $Nb_n C_6$.^{9,11} A detailed discussion of this difference is given in Sec. IV.

Two other very different ionization lasers (226 nm with 180 fs duration and 46.9 nm with ~ 1 ns duration) are used to verify that the dehydrogenation products are formed in the pickup cell and not in the ionization region through 193 nm photochemistry. The idea is that products with less (or at least different) dehydrogenation would be observed by femtosecond or very low energy/pulse ($< 1 \mu J/pulse$) x-ray laser ionization, if 193 nm laser ionization causes the dehydrogenation observed. No such products are observed in these two experiments. We believe that dehydrogenation products observed through low fluence 193 nm laser ionization in these studies are formed in the pickup cell.

Timing issues are found to be important in the pickup cell experiments. Figure 2 presents mass spectra for the reaction of Nb_n with benzene (~ 1 mTorr) obtained by ionization (193 nm) at different delay times with respect to the ablation event. This figure shows that the product distribution ($Nb_n C_6 H_x$) based on collision with one benzene molecule reaches the ionization region later than does the bare metal Nb_n cluster, and that $Nb_n C_{12} H_x$ arrives at the ionization region even later. This result is in quantitative agreement with the gas kinetic estimation that predicts a speed decrease

TABLE I. Products ($M_nC_xH_y$, $M=Nb$ and Ta , $n < 12$) observed in reactions of niobium and tantalum clusters with various unsaturated hydrocarbons in a pickup cell.

| n | Nb | | | | | Ta | |
|-----|--|-------------------------|------------------------|----------------------------|-----------------------|------------------------|-------------------------------------|
| | C_2H_2 0.77 mTorr | C_2H_4 0.77 mTorr | C_4H_6 0.68 mTorr | C_6H_6 0.98 mTorr | C_7H_8 1.4 mTorr | C_6H_6 0.85 mTorr | C_7H_8 1.4 mTorr |
| 1 | $x, y=2, 2; 4, 4; 6, 4$ all very weak | 2,2 (strong); 4,4 | 2,2; 4,4; 6,6 | 6,4; 6,6; 12,10 | 7,6 | 6,4; 6,6; 12,10 | 6,4; 6,6; 7,6 |
| 2 | 2,0; 4,2 | 2,2; 4,4 | 4,2; 4,4 | 6,4 very weak | 7,6 | | 7,4 |
| 3 | 2,0; 4,0 | 2,0; 2,2 (weak); 4,2 | 4,0; 4,2 | 6,2 | 7,2; 7,4 | 6,2 | 7,2 |
| 4 | 2,0; 4,0; 6,0 | 2,0; 4,0 | 4,0 | 6,0; 6,2 very weak | 7,2 | 6,0 | 5,0; 5,2; 6,0; 7,2 |
| 5 | 2,0; 4,0; 6,0 | 2,0; 4,0 | 4,0; 8,0 | 6,0 | 7,0; 7,2 | 6,0 | 6,0; 7,0 |
| 6 | 2,0; 4,0; 6,0 | 2,0; 4,0 | 4,0; 8,0 | 6,0 | 7,0 | 6,0 | 6,0; 7,0 |
| 7 | 2,0; 4,0; 6,0 | 2,0; 4,0; 6,0 | 4,0; 8,0 | 6,0; 12,0 | 7,0 | 6,0; 12,0 | 6,0; 7,0; 12,0; 13,0; 14,4 |
| 8 | 2,0; 4,0; 6,0 | 2,0; 4,0 all weak | 4,0; 8,0; 12,0 | 6,0; 6,6; 12,0 all weak | 7,0; 12,0 | 6,0; 12,0 | 6,0; 7,0; 11,0; 12,0; 14,2 |
| 9 | 2,0; 4,0; 6,0 | 2,0; 4,0; 6,0 | 4,0; 8,0; 12,0 | 6,0; 12,0 | 7,0; 12,2 | 6,0; 12,0 | 6,0; 7,0; 11,0; 12,0; 13,0; 14,2 |
| 10 | 2,0; 4,0; 6,0; 8,0 | 2,0; 4,0 all weak | 4,0; 8,0; 12,0 | 6,0; 12,0 all weak | 7,0; 12,0; 14,0 | 6,0; 12,0 | 6,0; 7,0; 11,0; 12,0; 13,0; 14,0 |
| 11 | 2,0; 4,0; 6,0; 8,0 | 2,0; 4,0; 6,0 | 4,0; 8,0; 12,0 | 6,0; 12,0 | 7,0; 14,0 | 6,0; 12,0 | 6,0; 7,0; 12,0; 13,0; 14,0 |

for Nb_n clusters if they collide with and pick up gas molecules in the reaction cell. This also eliminates the possibility that products are formed in the nozzle where a small amount of reactant gas might reside (10^{-6} Torr) due to background from the pickup cell. As shown in Fig. 2, the relative signal of products ($Nb_nC_xH_y$ and $Nb_nC_{12}H_y$) with respect to bare Nb_n depends significantly on the ionization laser delay time.

Based on the above experimental condition studies, the 193 nm laser fluence employed for all other reaction systems is kept below 1 mJ/cm^2 per pulse and typically is kept in the range of $100\text{--}400 \text{ }\mu\text{J/cm}^2$ per pulse depending on signal magnitude in the given experiment. The ablation/ionization laser time delay is also set (at “0 μs ” in Fig. 2) so that product features have the best signal/noise ratio. The results obtained under these experimental conditions are documented in Table I and presented in Figs. 3–6 and are explained below.

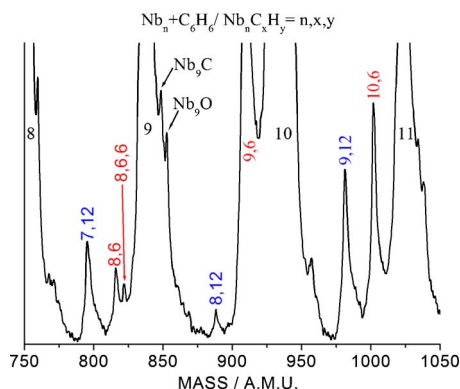


FIG. 3. Mass spectrum showing few products due to Nb_8 and Nb_{10} in the reaction of Nb_n with ~ 1 mTorr C_6H_6 in the pickup cell. Ionization is by a 193 nm laser with fluence of $190 \text{ }\mu\text{J/cm}^2$.

To emphasize the relatively low yield of product for Nb_8 and Nb_{10} clusters reacting with C_6H_6 , this region of the mass spectrum is expanded for the spectra of Figs. 1 and 2 and presented in Fig. 3. Note that one very low intensity nondehydrogenated product $Nb_8C_6H_6$ is identified in the spectrum. A comparison of the product distributions for Nb_n reacting with ethylene and acetylene in the mass regions Nb_7 to Nb_{11} is shown in Fig. 4. Products for Nb_8 and Nb_{10} reacting with C_2H_4 are of particularly low intensity; this is not true, however, for Nb_n reacting with C_2H_2 under the same conditions. In fact $Nb_{8,10}/C_{2,4,6,8}$ can all be identified in this reaction with C_2H_2 .

The reaction results for Ta_n reacting with various simple

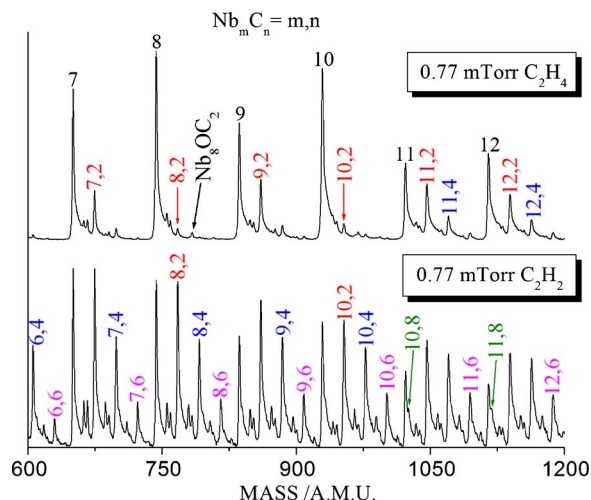


FIG. 4. Product distribution in the reaction of Nb_n with 0.8 mTorr C_2H_4 and C_2H_2 in the pickup cell. Ionization is by a 193 nm laser with fluence of $70 \text{ }\mu\text{J/cm}^2$.

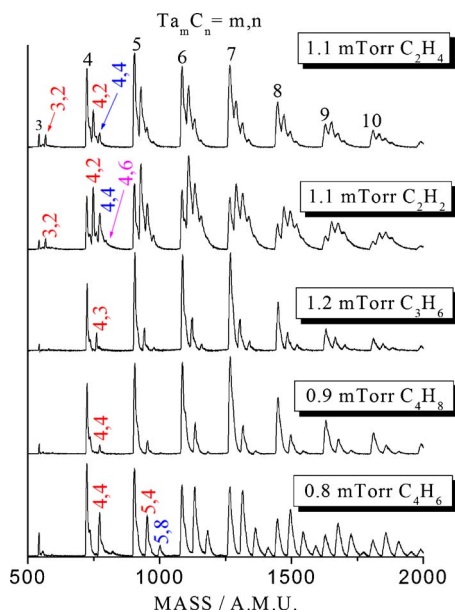


FIG. 5. Product distribution in the reaction of Ta_n with ethylene, acetylene, propylene, 1-butene, and 1,3-butadiene in the pickup cell. The vapor pressures of the hydrocarbons are indicated on the figure. Ionization is by a 193 nm laser with fluence of ~ 1 mJ/cm².

unsaturated hydrocarbons (acetylene, ethylene, propylene, 1-butene, 1,3-butadiene) are shown in Fig. 5. No strong size dependent reactivity is found for Ta_n in these reactions, and reactivity of Ta_n generally increases with increasing n . The reaction between Ta_n and hydrocarbons is more facile for the more unsaturated reactants (i.e., C_2H_2 and C_4H_6 generate more abundant products than the other reactants of Fig. 5).

The reaction products of Nb_n and Ta_n with toluene are presented in Fig. 6. Note that Nb_8C_{12} and Ta_8C_{12} are significant products in the reaction and that their signal magnitudes are intense among the carbon loss products such as $Nb_nC_{12}H_x$, Ta_nC_6 , Ta_nC_{12} , and Ta_nC_{13} . Table I lists the observed products ($M_nC_xH_y$, $n < 12$) for various reactions.

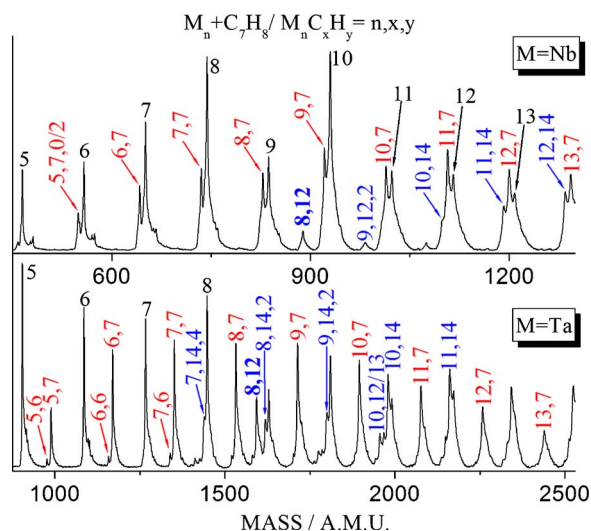


FIG. 6. Product distribution in the reaction of Nb_n and Ta_n with 1.4 mTorr toluene in the pickup cell. The vapor pressures of the hydrocarbons are indicated on the figure. Ionization is by a 193 nm laser with fluence of 770 mJ/cm².

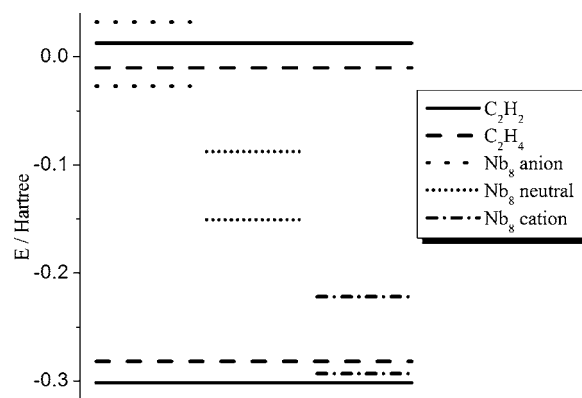


FIG. 7. Relative HOMO and LUMO positions of C_2H_2 , C_2H_4 , Nb_8 , and $Nb_8^{+/-}$. B3LYP/6-311+G(2d,p) method and basis set are used for C_2H_2 and C_2H_4 with the optimized structure. B3LYP/LANL2DZ are used for Nb_8 and its ions. The structure of Nb_8 is optimized (singlet multiplicity) and the same structure is used for the ions (doublet multiplicity).

IV. DISCUSSION

A. General

Nb_n and Ta_n neutral clusters readily react with unsaturated hydrocarbons under single collision condition, as shown in Figs. 1–6 and Table I. More dehydrogenation occurs for these neutral clusters as the cluster size increases and full dehydrogenation begins to occur for $2 \leq n \leq 5$, depending mainly on the degree of hydrocarbon unsaturation and number of hydrogen atoms contained. This result is in agreement with thermodynamic considerations that more metal carbon bonds can be formed as cluster size increases and more energy can be released to evaporate more hydrogen atoms from the product cluster. This trend is predicted by calculation for the reaction of C_2H_4 with Nb_n ;¹⁴ full dehydrogenation is thermodynamically allowed for $n \geq 3$. Several saturated hydrocarbons, such as methane, ethane, propane, n -butane, and cyclohexane are also used as reaction gases and no product is observed under our experimental conditions, although the reaction is thermodynamically allowed for a large cluster: for example, calculation in Ref. 14 and thermodynamic data of C_2H_4 and C_2H_6 show that $Nb_n + C_2H_6 \rightarrow Nb_nC_2 + 3H_2$ is allowed for $n \geq 6$. Figures 4 and 5 show that for the same experimental conditions, acetylene reacts more completely than ethylene with Nb_n and Ta_n neutral clusters, and that 1,3-butadiene reacts more completely than 1-butene with Ta_n neutral clusters. All these observations suggest that dehydrogenation of unsaturated hydrocarbons on neutral Nb_n and Ta_n clusters is initiated by the interaction of an unsaturated carbon-carbon bonding structure with the metal cluster.

In the language of frontier molecular orbital theory,³³ electron transfer or donation from (to) the π -HOMO (π^* -LUMO) of the unsaturated hydrocarbon to (from) the LUMO (HOMO) of the cluster initiates the formation of a π -bonded complex and causes the dehydrogenation reaction. An example of the relative lowest unoccupied molecular orbital (LUMO) and highest occupied molecular orbital (HOMO) positions for hydrocarbons and metal clusters is presented in Fig. 7. C_2H_2 and C_2H_4 have similar HOMO/LUMO positions relative to the neutral metal cluster Nb_8 . Because the HOMO and LUMO of C_2H_2 are both doubly

degenerate, the overlap between the frontier MOs of the metal cluster and C_2H_2 will be larger than that between the metal cluster and the nondegenerate MOs of C_2H_4 . This enables a larger π interaction between M_n and C_2H_2 than between M_n and C_2H_4 . Moreover, $[C_2H_2+H_2]$ is higher in energy than C_2H_4 and thus the reaction to form $(M_nC_2+H_2)$ from C_2H_2 is energetically more favorable than the reaction to form $(M_nC_2+2H_2)$ from C_2H_4 . These ideas suggest a more facile reaction between metal clusters and more unsaturated hydrocarbons than between metal clusters and less unsaturated hydrocarbons, particularly for C_2H_2 vs C_2H_4 and C_4H_6 vs C_4H_8 . Figure 7 also shows that the relative positions of the frontier MOs of the same metal cluster (Nb_8) in three different charge states are quite different. This may explain why reactivity of the Nb_8^- cluster anion is about one order of magnitude lower than that of the Nb_8^+ cluster cation for the dehydrogenation of benzene.²¹

B. Reaction of neutral Nb_n and Ta_n with benzene

Reaction of neutral Nb_n clusters with benzene has been studied in detail by fast flow (high pressure) experiments.⁹⁻¹¹ The primary products of these experiments are found to be only $Nb_nC_6H_6$ for $n < 3$, both Nb_nC_6 and $Nb_nC_6H_6$ for $n > 3$, and no dehydrogenation at all for secondary addition. Results for pickup cell (low pressure) reactions are presented in Figs. 1 and 2 and Table I for Nb_n and benzene. Clearly the present results are different from those reported in the literature. These differences can be anticipated and are listed below and possible explanations for them are given.

The first, and perhaps most noticeable difference between the flow tube and pickup cell results, is that except for $n=1$ and 8, all products have lost some hydrogen atoms for the pickup cell reaction. This is expected for a pickup cell experiment: these are low pressure reactions with no inert gas collisions to stabilize reaction intermediates and remove energy from the cluster reaction complex. Presumably the π -bonded initial activated collision complex ($Nb_n \cdots C_6H_6^*$) has association energy (~ 0.5 – 1.5 eV), center of mass kinetic energy (~ 0.3 eV), and an unknown initial cluster internal energy. Assuming that the cluster rotational and electronic temperatures are low, the internal energy can be estimated by the vibrational energy $E_v = (3n-6)kT_v = (n-2)0.077(T_v/T_0)$ eV, where k is the Boltzmann constant (8.617×10^{-5} eV/K), T_v is the vibrational temperature in Kelvin, and $T_0 = 298$ K. The fate of the activated complex $Nb_n \cdots C_6H_6^*$ in the pickup cell experiment is one of the following. For channel a, $Nb_n \cdots C_6H_6^*$ falls apart to the original reactants (Nb_n and C_6H_6) within one vibrational period (< 1 ps); For channel b, $Nb_n \cdots C_6H_6^*$ forms a dehydrogenation product (e.g., $Nb_nC_6 + 3H_2$) directly, also within one vibrational period time scale; and for channel c $Nb_n \cdots C_6H_6^*$ undergoes intracuster vibrational redistribution (IVR, < 1 ps) of energy (~ 0.8 – 1.8 eV) from the association coordinate to other degrees of freedom, such as Nb–Nb and Nb–C vibrations, and a metastable complex $Nb_nC_6H_6^*$ is formed. Channel b is unlikely because IVR must precede any bond breaking so we can ignore this possibility. One expects that IVR is fast enough to compete with channel a above, direct disso-

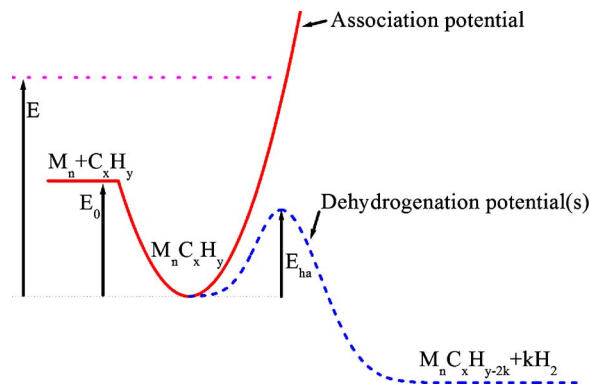


FIG. 8. A schematic diagram showing the potential curves that are involved in the association and dehydrogenation reaction of metal clusters with hydrocarbons. In the figure E is the total energy, E_0 is the association/binding energy, and E_{ha} is the energy of hydrogen activation. Vibrational coordinates that are involved in the association and dehydrogenation are different and the assumption that a double minimum potential along one coordinate exists in Ref. 25 may not be accurate.

ciation, otherwise no products would be observed. From the pressure of bath gas (1–50 Torr) in the flow tube reactor experiments,^{4,14} the collision rate for the cluster (Nb_{10} , $r \sim 4.5 \times 10^{-10}$ m) and the bath gas molecules (He, $r \sim 1 \times 10^{-10}$ m) is estimated to be $(0.02-1) \times 10^9$ s⁻¹. If roughly ten collisions (10–500 ns) are required to cool and stabilize the collision complex efficiently, formation of the metastable complex $Nb_nC_6H_6^*$ by IVR must also happen in the flow tube experiment, otherwise no direct association product would be observed. On the basis of the above observations and in agreement with the results for the cationic cluster system,²⁵ we conclude that the metastable association complex $Nb_nC_6H_6^*$ is formed in both the pickup and flow tube reactor cells.

Consider now the fate of the stabilized (by IVR) $Nb_nC_6H_6^*$ complex in the pickup cell experiment. For channel 1, energy is regained in the original association coordinate and the complex dissociates to Nb_n and C_6H_6 . The rate of dissociation (k_{dis}), in general, should decrease with increasing n according to the Rice-Ramsberger-Kassel-Markus (RRKM) theory (assuming all clusters Nb_n have the same vibrational temperature, which may not be true). k_{dis} at $n \sim 7-8$ would be in the order of 10^4 s⁻¹ if a $T_v \sim 298$ K is assumed. For channel 2, enough energy flows to a coordinate that aids hydrogen activation and causes dehydrogenation. If the hydrogen activation energy E_{ha} (see Fig. 8) is significantly larger than the $Nb_n \cdots C_6H_6$ association energy (E_0), the dehydrogenation product will have a small concentration: our pickup cell studies suggest that the dehydrogenation rate is faster than the dissociation rate (ca. 10^4 s⁻¹, $n > 5$, $n \neq 8, 10$) and thus the activation barrier is smaller than the association energy $E_{ha} < E_0$. Because comparable amounts of $Nb_nC_6H_6$ and Nb_nC_6 ($n > 5$, $n \neq 8, 10$) are formed in flow tube experiments,⁹⁻¹¹ the dehydrogenation rate in the low pressure pickup cell experiments must be comparable to the cooling rate due to bath gas in the high pressure flow tube reactor experiments which is 10^7-10^9 s⁻¹ for $n \sim 10$. For channel 3, a high activation barrier exists ($E_{ha} > E_0$) and $Nb_nC_6H_6^*$ remains bound for 50–100 μ s and is detected at

the ionization region. Finally, for channel 4, the complex is stabilized by collision or radiation and the $\text{Nb}_n\text{C}_6\text{H}_6$ complex is detected. In the pickup cell experiments this is not likely because the collision rate is small (one to three collisions per 50 μs), and radiative cooling through IR emission should require milliseconds. Thereby, channel 2 seems the most reasonable choice for a dual explanation of both low and high pressure studies of $\text{Nb}_n + \text{C}_6\text{H}_6 \rightarrow \text{Nb}_n\text{C}_6$ and $\text{Nb}_n\text{C}_6\text{H}_6$ ($n > 5$, $n \neq 8, 10$): $E_{\text{ha}} < E_0$ and the rate for dehydrogenation is $10^4 \leq k_{\text{dh}} \leq 10^7 - 10^9 \text{ s}^{-1}$.

The second difference between high pressure flow tube and low pressure pickup cell experiments is the appearance of products such as $\text{Nb}_2\text{C}_6\text{H}_4$, $\text{Nb}_3\text{C}_6\text{H}_2$, and $\text{Nb}_4\text{C}_6\text{H}_2$ observed at low pressure—at high pressure $\text{Nb}_n\text{C}_6\text{H}_6$ ($n=2, 3, 4$), is observed. The reason that these partially dehydrogenated products are not observed for the fast flow experiment is that collisions with the bath gas cool the association products much faster than the dehydrogenation reaction can occur for these small clusters. These small clusters must have low vibrational energy under high pressure conditions and may have a relatively high dehydrogenation activation energy.

The third difference between high and low pressure experiments with regard to product generation deals with addition of a second unsaturated hydrocarbon to the initial activated complex, to form products Nb_nC_{12} , that are fully dehydrogenated, as observed for $n \geq 7$ in the pickup cell experiment. The corresponding products for the flow tube reactor experiments are $\text{Nb}_n\text{C}_{12}\text{H}_6$ and $\text{Nb}_n\text{C}_{12}\text{H}_{12}$.¹¹ These products are suggested to arise due to passivation of the clusters toward further dehydrogenation once the primary addition products (Nb_nC_6 and $\text{Nb}_n\text{C}_6\text{H}_6$) are formed. The results from the present low pressure pickup cell studies shed new light on these high pressure flow tube results. In the first instance, for formation of $\text{Nb}_n\text{C}_{12}\text{H}_6$, dehydrogenation is not favored because collisions cool the cluster Nb_nC_6 to the level that $\text{Nb}_n\text{C}_{12}\text{H}_6$ does not have enough residual energy to surmount the activation barrier to further dehydrogenation in the reaction $\text{Nb}_n\text{C}_{12}\text{H}_6 \rightarrow \text{Nb}_n\text{C}_{12} + 3\text{H}_2$. In the second instance, for the formation of $\text{Nb}_n\text{C}_{12}\text{H}_{12}$, due to the addition of C_6H_6 to $\text{Nb}_n\text{C}_6\text{H}_6$, both reactant and product clusters ($\text{Nb}_n\text{C}_6\text{H}_6$ and $\text{Nb}_n\text{C}_{12}\text{H}_{12}$) are cooled fast enough through collisions with bath gas that neither activation barrier to H_2 loss can be surmounted. Thus the observation of hydrogenated products in the high pressure experiments may be attributed to the reduced cluster temperature due to collisional cooling.

The high temperature of Nb_nC_6 in the low pressure pickup cell experiment may be responsible for the observation of NbC_6H_4 and NbC_6H_6 (see Table I and Figs. 1 and 2). In these experiments the cluster formation conditions can be controlled such that only Nb atom ($n=1$) is present in the molecular beam. In this instance, NbC_6H_4 and NbC_6H_6 cannot be observed. Note that these species in Fig. 2 only appear at later time delays for which larger Nb_n clusters are present. Moreover, the formation of $\text{NbC}_6\text{H}_4 + \text{H}_2$ from $\text{Nb} + \text{C}_6\text{H}_6$ may not be energetically favorable and it may not be possible for the small direct association complex NbC_6H_6 to survive 50–100 μs for detection. One possibility for the generation

of these two species, NbC_6H_4 , and NbC_6H_6 , is through the reactions $\text{Nb}_n + \text{C}_6\text{H}_6 \rightarrow \text{Nb}_{n-1} + \text{NbC}_6\text{H}_6$ ($n > 1$) and $\text{Nb}_n + \text{C}_6\text{H}_6 \rightarrow \text{Nb}_{n-1} + \text{NbC}_6\text{H}_4 + \text{H}_2$. The fragmentation energy of $\text{Nb}_n \rightarrow \text{Nb}_{n-1} + \text{Nb}$, however, is above 4.5 eV.³⁴ The calculated association energy for $\text{Nb} + \text{C}_6\text{H}_6 \rightarrow \text{NbC}_6\text{H}_6$ is only 1.5 eV.²⁹ This gives the initial vibrational energy of Nb_n to be at least $4.5 - 1.5 - 0.3 \text{ eV} = (\text{bonding energy}) - (\text{association energy}) - (\text{center of mass kinetic energy}) = 2.7 \text{ eV}$, corresponding to $T_v = 1306 \text{ K}$ for $n=10$, if $\text{Nb}_n + \text{C}_6\text{H}_6 \rightarrow \text{Nb}_{n-1} + \text{NbC}_6\text{H}_6$ happens. The actual vibrational energy would be even higher than this value if the reaction happens within 50–100 μs . Note that VO_2 has been determined to have a vibrational temperature of ca. 700 K under collision-free conditions following supersonic expansion.³⁵ Additionally, a more reasonable mechanism for the low pressure formation of NbC_6H_6 might be $\text{Nb}_n\text{C}_6 + \text{C}_6\text{H}_6 \rightarrow \text{Nb}_{n-1}\text{C}_6 + \text{NbC}_6\text{H}_6$, as Nb_nC_6 can be hotter than $\text{Nb}_n\text{C}_6\text{H}_6$ due to the dehydrogenation reaction energy. Both paths are apparently possible based on thermal considerations.

In addition to the differences mentioned above between the pickup cell and flow tube reactor results which can be explained by the cooling effect of the high pressure reactions, we also notice good agreement between the results of this work and those of previous studies. Figure 1 shows that the mass spectral signals for the products Nb_8C_6 and Nb_{10}C_6 are relatively low in the pickup experiment: Nb_8 and Nb_{10} are particularly unreactive toward dehydrogenation of benzene. This has been previously observed by fast flow reactor experiments and suggests that the cluster temperature in this work is not very high compared to that of the previous studies. The low reactivity of Nb_8 and Nb_{10} in benzene dehydrogenation can be rationalized by considering a relatively high hydrogen activation ($E_{\text{ha}} > E_0$ in Fig. 8) in the particular systems. Thus, the low reactivity of Nb_8 and Nb_{10} toward benzene need not be caused by thermodynamic considerations but by kinetic problems due to high activation barriers for the reactions. This supposition is supported by the fact that Nb_8 and Nb_{10} react with C_2H_2 , C_7H_8 , and C_4H_6 molecules to form Nb_8C_6 , Nb_8C_7 , and Nb_8C_8 much more readily than Nb_8C_6 forms from $\text{Nb}_8 + \text{C}_6\text{H}_6$. Nb_8 and Nb_{10} are also found to be unreactive with D_2 and N_2 ,⁵ but this may be partially due to high ionization energies³⁶ and high HOMO/LUMO gaps^{37,38} of the clusters. In these various instances of specific reactivity, we suggest that the overall cluster Nb_n and its reactant gas partner (C_6H_6 , C_2H_4 , C_4H_6 , etc.) must be considered as a reaction unit (see Figs. 4 and 5).

The results for benzene dehydrogenation on neutral Nb_n clusters in the pickup cell experiments discussed in this report are also similar in many ways to the data obtained in FT-ICR experiments on cationic Nb_n clusters. In these latter experiments, the same partially dehydrogenated stoichiometry for small product clusters (e.g., $\text{Nb}_2\text{C}_6\text{H}_4^+$, $\text{Nb}_3\text{C}_6\text{H}_2^+$, and $\text{Nb}_4\text{C}_6\text{H}_2^+$) is observed. Full dehydrogenation occurs for Nb_n^+ with C_6H_6 for $n > 5$. All second collision products are found to be completely dehydrogenated as well, in the FT-ICR studies. Because single collision low pressure conditions are employed in both the pickup and FT-ICR experiments, this product similarity for both cases indicates that charge does not significantly alter the reaction energetics. Anionic clus-

ters also behave and react in a similar fashion.²¹ Nonetheless, for relatively low reactivity systems, charge does seem to matter in the cluster dehydrogenation reaction with benzene. Refs. 16 and 21 show that products $\text{Nb}_{12}\text{C}_6^+$, $\text{Nb}_{13}\text{C}_6^-$, $\text{Nb}_{17}\text{C}_6^-$, $\text{Nb}_{19}\text{C}_6^{+-}$, and $\text{Nb}_{22}\text{C}_6^{+-}$ are of relatively low concentration but $\text{Nb}_8\text{C}_6^{+-}$ and $\text{Nb}_{10}\text{C}_6^{+-}$ are not. This charge dependent low reactivity (at least for $n < 19$) suggests that electronic rather than geometric structural properties in these particular systems are responsible for the barriers to dehydrogenation.

$\text{Nb}_n\text{C}_6\text{H}_6^{+-}$ ionic clusters are detected in the FT-ICR experiment for cluster size in the range of $12 < n < 22$. As shown in Fig. 3, a low intensity signal is observed for $\text{Nb}_8\text{C}_6\text{H}_6$ for the pickup cell low pressure experiment. This is consistent with the interpretation that the hydrogen activation barrier in this system is relatively high so that the metastable complex $\text{Nb}_8\text{C}_6\text{H}_6^*$ cannot accumulate sufficient energy to surmount this barrier within 50–100 μs . These data also suggest that the T_v of the cluster is not very high, otherwise the lifetime of the metastable $\text{Nb}_8\text{C}_6\text{H}_6^*$ would be short and the cluster could not be observed. The observation of this product coupled with RRK theory may be used to estimate T_v of the clusters generated in this work. Because a small amount of $\text{Nb}_8\text{C}_6\text{H}_6^*$ (about 5%, using the peak intensity ratio of $\text{Nb}_8\text{C}_6\text{H}_6$ to Nb_9C_6 in Fig. 3) can survive on average about 75 μs for detection, the lifetime of $\text{Nb}_8\text{C}_6\text{H}_6^*$ is estimated to be 25 μs . This corresponds to a dissociation rate constant k_{dis} ($\text{Nb}_8\text{C}_6\text{H}_6^* \rightarrow \text{C}_6\text{H}_6 + \text{Nb}_8$) = $4 \times 10^4 \text{ s}^{-1}$. In RRK theory, $k_{\text{dis}} = \nu (1 - E_0/E)^{3n-7}$, in which ν is the effective frequency of the $\text{Nb}_8 \cdots \text{C}_6\text{H}_6$ reaction coordinate vibration ($\nu = 3 \times 10^{12} \text{ s}^{-1}$, $\sim 100 \text{ cm}^{-1}$ is assumed), E_0 is the association energy (0.5–1.5 eV), E is the total energy (see Fig. 8) and $E = E_0 + E_k + E_v \sim (E_0 + 0.3 + 0.462T_v/298) \text{ eV}$ and C_6H_6 is treated as one unit and $n = 8 + 1 = 9$ is used. We find $E/E_0 = 1.68$ and $T_v = 245$ and 464 K for $E_0 = 1.0$ and 1.5 eV, respectively. These are acceptable values of temperature prior to reaction considering that some supersonic cooling exists for these experiments. If T_v is increased to 1300 K, $k_{\text{dis}} \sim 2.3 \times 10^9 \text{ s}^{-1}$ ($E_0 = 1 \text{ eV}$) and $1.4 \times 10^8 \text{ s}^{-1}$ ($E_0 = 1.5 \text{ eV}$). This temperature would not be consistent with a $\text{Nb}_8\text{C}_6\text{H}_6$ product being observed.

C. Reaction with ethylene

In general, considerations of the preceding subsection on benzene reactions with Nb_n can be employed to explain experimental results for the dehydrogenation reaction of various unsaturated hydrocarbons on Nb_n and Ta_n neutral clusters. Since ethylene dehydrogenation on niobium neutral and ionic clusters is also extensively studied by fast flow (high pressure) and FT-ICR (low pressure) experiments,^{14,16,19} a comparison between the present pickup cell results and those previous studies is emphasized in this subsection.

As shown in Fig. 4 and Table I, all primary and sequential addition products in reactions of C_2H_4 with Nb_n are fully dehydrogenated for $n > 3$. Thus, full dehydrogenation is both thermodynamically and kinetically (50–100 μs) favorable for clusters $[\text{Nb}_n(\text{C}_2\text{H}_4)_x, n > 3]$ with internal temperatures between 250 and 460 K. Nonetheless, most primary (e.g.,

$n = 8-12, 14-25$) and sequential addition products for flow tube experiments¹⁴ are only partially dehydrogenated. This observation suggests that more than one step is involved in the dehydrogenation process (such as $\text{Nb}_9\text{C}_2\text{H}_4 \rightarrow \text{Nb}_9\text{C}_2\text{H}_2 + \text{H}_2$ and $\text{Nb}_9\text{C}_2\text{H}_2 \rightarrow \text{Nb}_9\text{C}_2 + \text{H}_2$), and that the rate of the second step is considerably slower than that of the first for both thermodynamic and kinetic reasons. An interesting difference between the fast flow experiments for the reaction of Nb_n clusters with C_2H_4 and C_6H_6 is that essentially no non-dehydrogenated products ($\text{Nb}_n\text{C}_2\text{H}_4, n \neq 10$) are observed for the C_2H_4 reaction, whereas nondehydrogenated products $\text{Nb}_n\text{C}_6\text{H}_6$ are observed for the C_6H_6 reaction. This implies that E_{ha} (Fig. 8) is relatively smaller for Nb_n with C_2H_4 than it is for Nb_n with C_6H_6 . Another possible explanation for these observations is that the bath gas pressure (~ 1 Torr) in the experiment with C_2H_4 (Ref. 14) is considerably lower than that (~ 50 Torr) in the experiment with C_6H_6 .^{4,9-11} As a result, the cooling in the C_2H_4 reaction with Nb_n is not as facile as that in the C_6H_6 reaction. This yields a dehydrogenation rate in the pickup experiment of $k_{\text{dh}} \sim 2 \times 10^7 \text{ s}^{-1}$ for $n \sim 10$, in agreement with previous estimation.

As shown in Fig. 4, Nb_8 and Nb_{10} are relatively unreactive with C_2H_4 , as has been reported for high pressure flow tube reactor experiments, for which the depletion rates for these two clusters are relatively very small. Recall that the depletion rates for Nb_8 and Nb_{10} with C_6H_6 are not relatively small.¹¹ These two observations can be explained based on the relatively higher values of E_{ha} than E_0 (see Fig. 8) and the poor cooling efficiency for the flow tube high pressure $\text{Nb}_n + \text{C}_2\text{H}_4$ reaction. An alternate explanation for these observations is that E_0 is particularly small for $\text{Nb}_8 \cdots \text{C}_2\text{H}_4$ and $\text{Nb}_{10} \cdots \text{C}_2\text{H}_4$ so that direct dissociation rate k_{dis} is large and the cooling is not fast enough to stabilize the association products. A small E_0 may also be responsible for the low reactivity for Nb_n and $\text{C}_m\text{H}_{2m+2}/c\text{-C}_m\text{H}_{2m}$ found both in these experiments and high pressure ones.⁸

As discussed previously, frontier molecular orbital interactions between M_n ($M = \text{Nb}$ and Ta) and saturated hydrocarbons are weaker than those for unsaturated hydrocarbons, and E_0 is also smaller for saturated hydrocarbon interactions with M_n clusters. Assuming ν and n are the same in the RRK rate formula,

$$\frac{k_{\text{dis}}^{\text{sat}}}{k_{\text{dis}}^{\text{usat}}} = \left(\frac{E_0^{\text{usat}} + \Delta E}{E_0^{\text{sat}} + \Delta E} \right)^{3n-7},$$

in which $\Delta E = E - E_0 \sim 0.3 + (n-2)(0.077 \text{ eV})$ for $T_v = 298 \text{ K}$. Using $E_0^{\text{sat}} = 0.38 \text{ eV}$ [n -butane with $\text{Ni}(111)$ surface³⁹], $E_0^{\text{usat}} = 1.0 \text{ eV}$, and $n = 10$, we find $k_{\text{dis}}^{\text{sat}}/k_{\text{dis}}^{\text{usat}} = (1.478)^{23} \sim 8 \times 10^3$. This implies that direct dissociation can be much faster for low binding energy systems than for high binding energy systems and thus saturated hydrocarbons may not have sufficient time as an activated complex with M_n to convert to product $M_n\text{C}_x\text{H}_y$ before dissociation.

Comparing results of neutral Nb_n cluster reactions with C_2H_4 in the present pickup cell experiment with those of cationic Nb_n clusters with C_2H_4 studied by FT-ICR,^{16,19} general agreement is again found between the neutral systems studied in this work and the charged systems reported in the literature: fully dehydrogenated products are observed for

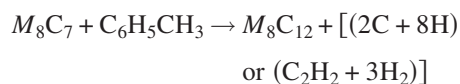
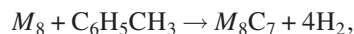
$n > 3$ for primary and secondary additions. In the case of low reactivity, Nb_{10}^+ and Nb_{12}^+ are particularly unreactive, while for the neutral system, Nb_8 and Nb_{10} are unreactive (Fig. 4).

D. Reaction with toluene

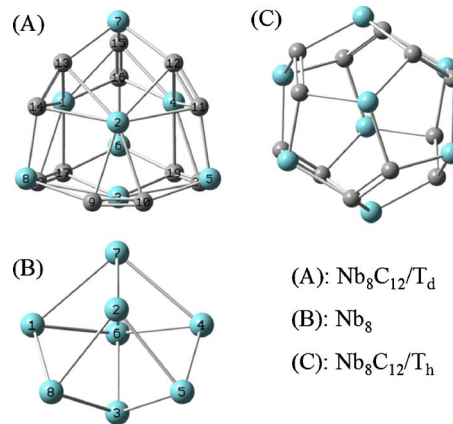
Reaction of M_n ($M=\text{Nb}$ and Ta) with $\text{C}_6\text{H}_5\text{CH}_3$ in this pickup cell experiment is interesting and the product distribution is shown in Fig. 6. In addition to the major dehydrogenation products such as $M_n\text{C}_7$ and $M_n\text{C}_{14}$, some less intense carbon loss species are observed, especially for Ta_nC_6 for $n > 4$ (see Table I). This observation implies that methyl group or methane loss is another reaction open channel for toluene plus Ta_n . Similar observations have also been made for a fast flow reactor system⁴⁰ in which losses of CO , CH_3 , H_2CO , and CH_3OH are observed for Nb_n reactions with appropriate benzene derivatives and unsaturated nonaromatic hydrocarbons. The carbon loss reaction channel is also identified in a few instances in FT-ICR reactions,¹⁶ such as $\text{Nb}_4^+ + \text{C}_6\text{H}_6 \rightarrow \text{Nb}_4\text{C}_5\text{H}^+ + \text{H}_2 + \text{CH}_3$, and reaction of Nb_n^+ with several propylene or 1-butene molecules.²⁰ The reaction of cationic Nb_n with toluene has also been studied by FT-ICR experiments,^{16,17} but no carbon loss products, such as $\text{Nb}_8\text{C}_{12}^+$, are reported.

Figure 6 demonstrates that among the carbon loss products for the reaction of M_n with toluene (Nb_nC_{12} , $\text{Nb}_n\text{C}_{12}\text{H}_2$, and Ta_nC_m with $m=5, 6, 11, 12, 13$), Nb_8C_{12} and Ta_8C_{12} are particularly abundant. We suggest that the “magic” Nb_8C_{12} and Ta_8C_{12} observed in the low pressure pickup cell experiment have the Met-Car structure³¹ that is generated for $M_8\text{C}_{12}$ ($M=\text{Ti}, \text{Zr}, \text{Hf}, \text{V}, \text{Nb}$) formed in the reaction of high temperature laser ablated metal plasma with seeded hydrocarbons in a carrier gas.³⁰ In these previous experiments,^{41,42} Ta_8C_{12} is reported to be not magic. This absence of the tantalum Met-Car species has been explained as due to a large Ta-Ta binding energy with respect to other metals;⁴³ however, observation of magic Ta_8C_{12} and also Nb_8C_{12} near the room temperature reaction of M_8 with toluene in the present study indicates that the failure to observe Met-Car Ta_8C_{12} in the laser ablation plasma experiments is probably due to kinetic constraints for this particular system. Ta_8C_{12} seems as stable as other Met-Cars generated in the pickup cell reaction.

Because the M_n ($M=\text{Nb}, \text{Ta}$) cluster dissociation energy is high (>4.5 eV for Nb_n),³⁴ we propose that $M_8\text{C}_{12}$ is formed directly from M_8 , although the possibility of its formation through metal fragmentation cannot be specifically excluded. The reaction pathways



may be used to interpret how the Met-Car is formed and thus reveal its topological structure. Figure 9 shows possible paths to form Nb_8C_{12} from Nb_8 by absorbing two toluene molecules. In this figure, structure (B) is a calculated Nb_8 structure (B3LYP/LANL2DZ) that is close to the Nb_8 structures of Ref. 38, and structures (A) and (C) are Nb_8C_{12} struc-



(A): $\text{Nb}_8\text{C}_{12}/T_d$
(B): Nb_8
(C): $\text{Nb}_8\text{C}_{12}/T_h$

FIG. 9. Structures of Nb_8 (B) and Nb_8C_{12} in T_d (A) and T_h (C) symmetries. The structure of Nb_8 is the optimized result by the B3LYP/LANL2DZ method and basis set (singlet multiplicity). Nb_8C_{12} in T_d and T_h symmetries is constructed according to the calculated structure of Ti_8C_{12} in Ref. 31. The view angles are arranged so that each niobium atom is in a similar position in the different molecules. Light blue = Nb; gray = C.

tures arranged in T_d and T_h symmetries, respectively. Inspection of these structures leads one to the conclusion that structure (A) is more readily formed from (B) than is (C) by absorbing two toluene molecules: (1) carbons [9,10], [11,12], and [13,14] can come from the benzene group and carbon [15] from the methyl group of the primary addition toluene; and (2) carbon [16] can come from the methyl group and carbons [17,18] and [19,20] from the benzene group of the second toluene molecule by fragmenting one CC unit in the secondary addition. We suggest that the second toluene is the species fragmented because the cluster complex $M_8\text{C}_6$ is not or only weakly observed. Our observation of Met-Car formation in the pickup cell experiment strongly supports the theoretical Met-Car T_d structure³¹ or at least disagrees with the original T_h structure⁴⁴ suggestion.

E. Comparison to surface catalytic reactions

One of the more interesting aspects of the present cluster gas phase reactions is that they parallel similar behavior found for clean metal surfaces, such as various Ni and Pt surfaces.^{45,46} In general, we have found that the reactivity of neutral metal cluster M_n toward unsaturated hydrocarbons is not dependent on cluster size n (geometric structure), rather cluster reactivity seems to correlate best to HOMO/LUMO electronic structure with regard to both the metal and the particular unsaturated hydrocarbon of interest, and reactant cluster “vibrational” temperature. To the extent that cluster and surface chemistries are similar, we suggest that surface electronic state energies relative to unsaturated hydrocarbon HOMO/LUMO energies are an important feature for surface/catalytic reactivity. Additionally, both local surface temperature and thermal dissipation (“IVR” and “collisional energy loss”) into the phonons of the condensed phase system also play major roles in the ability of metal surfaces to support dehydrogenation reactions for unsaturated hydrocarbons.

V. CONCLUSIONS

The initial step in the reaction of neutral metal clusters M_n ($M=Nb, Ta$) with unsaturated hydrocarbons (C_xH_y) is the formation of a metastable complex $M_nC_xH_y^*$. This conclusion comes from a detailed comparison of reaction products arising from both pickup cell (low pressure) and flow tube reactor (high pressure) experiments. These results, in conjunction with RRK theory of reaction rate constants, yield information on a number of basic concepts for neutral metal cluster/unsaturated hydrocarbon reactions: (1) the barrier to hydrogen activation, (2) rates of dehydrogenation, direct dissociation, and cooling of the clusters and cluster complexes by bath gas collisions for flow tube experiments, (3) cluster temperature, and (4) thermodynamic and kinetic control of reaction pathways.

The major products in this pickup experiment are fully dehydrogenated, in contrast to flow tube reactor high pressure results for which non- and partial dehydrogenation reactions often occur. This product difference at high and low pressures is due to the cooling effect of collisions between the reaction complex $M_nC_xH_y^*$ and bath gas for the flow tube experiments. This cooling effect implies a complicated situation for the dehydrogenation reaction on the surface of a metal for which phonon modes can substitute for bath gas collisions.

Neutral and ionic clusters have a surprising similarity in extent of dehydrogenation (loss of the number of H_2 molecules), indicating that the charge does not change the overall thermodynamics and mechanisms significantly. Nonetheless, neutral and ionic clusters behave quite differently in low reactivity situations such as Nb_8 and Nb_{10} with both C_2H_4 and C_6H_6 , and Nb_{10}^+ and Nb_{12}^+ (not Nb_8^+) with C_2H_4 . This suggests that the barriers in these particular reactions strongly depend on cluster charge and that electronic state properties rather than structural properties cause low cluster reactivity for a particular reaction. Nb_8C_{12} and Ta_8C_{12} are synthesized in metal cluster reactions with unsaturated hydrocarbons C_6H_6 and $C_6H_5CH_3$ in a pickup cell. Such a synthesis supports two hypotheses: (1) a T_d structure for M_8C_{12} and (2) generation of Met-Cars from near room temperature metal nanopowder rather than laser ablated metal or metal carbide plasmas should be possible.

ACKNOWLEDGMENTS

This work was supported by Philip Morris, USA, the U.S. DOE BES program, and the NSF ERC for Extreme Ultraviolet Science and Technology under NSF Award No. 0310717.

¹M. B. Knickelbein, *Annu. Rev. Phys. Chem.* **50**, 79 (1999).

²P. B. Armentrout, *Annu. Rev. Phys. Chem.* **52**, 79 (2001).

³T. G. Dietz, M. A. Duncan, D. E. Powers, and R. E. Smalley, *J. Chem. Phys.* **74**, 6511 (1981).

⁴M. E. Geusic, M. D. Morse, S. C. O'Brien, and R. E. Smalley, *Rev. Sci. Instrum.* **56**, 2123 (1985).

⁵M. D. Morse, M. E. Geusic, J. R. Heath, and R. E. Smalley, *J. Chem. Phys.* **83**, 2293 (1985).

⁶J. L. Persson, M. Andersson, and A. Rosén, *Z. Phys. D: At., Mol. Clusters* **26**, 334 (1993).

⁷M. Andersson, J. L. Persson, and A. Rosén, *J. Phys. Chem.* **100**, 12222 (1996).

⁸R. J. St. Pierre, E. L. Chronister, L. Song, and M. A. El-Sayed, *J. Phys. Chem.* **91**, 4648 (1987).

⁹R. J. Pierre and M. A. El-Sayed, *J. Phys. Chem.* **91**, 763 (1987).

¹⁰R. J. Pierre and M. A. El-Sayed, *J. Phys. Chem.* **91**, 5228 (1987).

¹¹M. R. Zakin, D. M. Cox, and A. Kaldor, *J. Phys. Chem.* **91**, 5224 (1987).

¹²M. R. Zakin, R. O. Brickman, D. M. Cox, and A. Kaldor, *J. Chem. Phys.* **88**, 5943 (1988).

¹³R. D. Laflaur, J. M. Parnis, and D. M. Rayner, *J. Chem. Phys.* **105**, 3551 (1996).

¹⁴J. M. Parnis, E. Escobar-Cabrera, M. G. K. Thompson, J. P. Jacula, R. D. Laflaur, A. Guevara-Garcia, A. Martinez, and D. M. Rayner, *J. Phys. Chem. A* **109**, 7046 (2005).

¹⁵Q.-F. Wu, W.-Y. Lu, and S.-H. Yang, *J. Chem. Phys.* **109**, 8935 (1998).

¹⁶C. Berg, T. Schindler, G. Niedner-Schatteburg, and V. E. Bondybey, *J. Chem. Phys.* **102**, 4870 (1994).

¹⁷C. Berg, T. Schindler, A. Lammers, G. Niedner-Schatteburg, and V. E. Bondybey, *J. Phys. Chem.* **99**, 15497 (1995).

¹⁸C. Berg, T. Schindler, M. Kantlehner, G. Niedner-Schatteburg, and V. E. Bondybey, *Chem. Phys.* **262**, 143 (2000).

¹⁹C. Q. Jiao and B. S. Freiser, *J. Phys. Chem.* **99**, 10723 (1995).

²⁰C. Q. Jiao, D. R. A. Ranatunga, and B. S. Freiser, *J. Phys. Chem.* **100**, 4755 (1996).

²¹C. Berg, M. Beyer, U. Achatz, S. Joos, G. Niedner-Schatteburg, and V. E. Bondybey, *J. Chem. Phys.* **108**, 5398 (1998).

²²D. B. Pedersen, J. M. Parnis, R. D. Laflaur, and D. M. Rayner, *J. Phys. Chem. A* **108**, 2682 (2004).

²³Y. M. Hamrick and M. D. Morse, *J. Phys. Chem.* **93**, 6494 (1989).

²⁴M.-C. Tsai, C. M. Friend, and E. L. Muetterties, *J. Am. Chem. Soc.* **104**, 2539 (1982).

²⁵V. E. Bondybey and M. K. Beyer, *J. Phys. Chem. A* **105**, 951 (2001).

²⁶F. Meyer, F. A. Khan, and P. B. Armentrout, *J. Am. Chem. Soc.* **117**, 9740 (1995).

²⁷J. Pawela-Crew and R. J. Madix, *Surf. Sci.* **339**, 8 (1995).

²⁸J. A. Connor, H. A. Skinner, and Y. Virmani, *J. Chem. Soc., Faraday Trans. 1* **68**, 1754 (1972).

²⁹S. Roszak, D. Majumdera, and K. Balasubramaniana, *J. Phys. Chem. A* **103**, 5801 (1999).

³⁰B. D. Leskivi and A. W. Castleman, Jr., *C. R. Phys.* **3**, 251 (2002), and references therein.

³¹M.-M. Rohmer, M. Bénard, and J.-M. Poblet, *Chem. Rev. (Washington, D.C.)* **100**, 495 (2000).

³²D. N. Shin, Y. Matsuda, and E. R. Bernstein, *J. Chem. Phys.* **120**, 4150 (2004).

³³K. Fukui, T. Yonezawa, and H. Shingu, *J. Chem. Phys.* **20**, 722 (1952).

³⁴D. A. Hales, L. Lian, and P. B. Armentrout, *Int. J. Mass Spectrom. Ion Process.* **102**, 269 (1990).

³⁵Y. Matsuda and E. R. Bernstein, *J. Phys. Chem. A* **109**, 3803 (2005).

³⁶R. L. Whetten, M. R. Zakin, D. M. Cox, D. J. Trevor, and A. Kaldor, *J. Chem. Phys.* **85**, 1697 (1986).

³⁷H. Kietzmann, J. Morenzin, P. S. Bechthold, G. Gantefor, and W. Eberhardt, *J. Chem. Phys.* **109**, 2275 (1998).

³⁸V. Kumar and Y. Kawazoe, *Phys. Rev. B* **65**, 125403 (2002).

³⁹C.-L. Kao and R. J. Madix, *Surf. Sci.* **557**, 215 (2004).

⁴⁰L. Song and M. A. El-Sayed, *J. Phys. Chem.* **94**, 7907 (1990).

⁴¹S. F. Cartier, B. D. May, and A. W. Castleman, Jr., *J. Am. Chem. Soc.* **116**, 5295 (1994).

⁴²H. T. Deng, B.-C. Guo, K. P. Kerns, and A. W. Castleman, Jr., *Int. J. Mass Spectrom. Ion Process.* **138**, 275 (1994).

⁴³S. F. Cartier, B. D. May, and A. W. Castleman, Jr., *J. Phys. Chem.* **100**, 8175 (1996).

⁴⁴B.-C. Guo, K. P. Kerns, and A. W. Castleman, Jr., *Science* **255**, 1411 (1992).

⁴⁵P. H. Holloway and J. B. Hudson, *Surf. Sci.* **43**, 123 (1974).

⁴⁶T. Fink, J. P. Dath, M. R. Bassett, R. Imbihl, and G. Ertl, *Surf. Sci.* **245**, 96 (1991).